Preprints of the 19th World Congress
The International Federation of Automatic Control
Cape Town, South Africa. August 24-29, 2014

Observability Analyses and Trajectory Planning for Tracking of an Underwater Robot using Empirical Gramians[1]

Thomas Glotzbach*, Naveena Crasta*, Christoph Ament*

** Institute for Automation and Systems Engineering, Technische Universität Ilmenau, 98684 Ilmenau, Germany (Tel: +49 3677 694107; e-mail: {thomas.glotzbach; naveena.crasta; christoph.ament }@tu-ilmenau.de)*

Abstract: In marine robotics, estimation of the position and orientation of an underwater agent requires lots of research efforts. Especially the realization of robot teams has opened new horizons, allowing for relative navigation based on relative range measurements between the agents. Hence, there is the need for a better understanding of optimal sensor placement related to the positions of the robots relative to each other, and for improvement of observability, based on the concrete mission scenario. In this paper, we study the tracking of a moving target by a Reference Objects (RO) capable of performing acoustic range measurements. We employ the well-known theory of the Empirical Gramians, to evaluate different scenarios and their influence on the observability properties. Emphasis will be put on the computation of a trajectory for the RO that optimizes the observability criterion. We will compare our results with others found in literature that were derived by different procedures, to proof the usability of the Empirical Gramian approach for the area of underwater robotics.

Keywords: Marine Robotics, Underwater Navigation, Observability Analyses, Trajectory Planning, Optimization, Empirical Gramians

1. INTRODUCTION

In the current research on underwater robotics, navigation plays a key role. We refer to navigation as the task of estimating the position and pose of a marine target, which is a precondition to almost all mission scenarios, as it influences both the control algorithms, which need navigation data as input, and many applications, e.g. geo-referencing. Underwater navigation is hindered by several issues, mainly the absence of a global positioning system underwater, the fact that inertial navigation sensors like Attitude Heading Reference Systems (AHRS) exhibit an error that grows over time, and the extremely low bandwidth and high error rate of acoustic communication systems that are used to measure distances underwater.

In the European research project MORPH, a group of European experts in marine robotics aim for the realisation of a so-called MORPH Supra-Vehicle (MSV) that consist of several autonomous marine robots, referred as nodes. Being not physically, but logically linked, these nodes are equipped with heterogeneous sensors and are expected to gain new abilities, like the cooperative mapping of vertical and overhanging cliff walls, as depicted in Fig. 1. More details can be found in Kalwa *et al*., 2012.

The requirements within MORPH, like different marine robots operating in close vicinity and the need to geo-reference mappings that are recorded over unstructured terrain, are driving our efforts to develop new strategies for cooperative navigation and to improve our knowledge on possible navigation procedures. Acoustic based range measurements between underwater agents and surface objects with access to a global positioning system, so called Reference Objects (ROs), play an important role in underwater navigation. Range information between the target

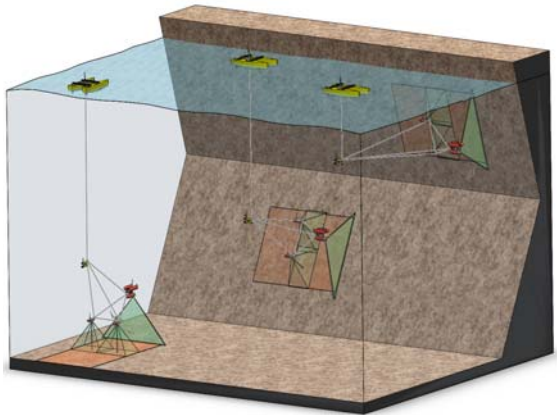

Fig. 1: The overall concept of MORPH

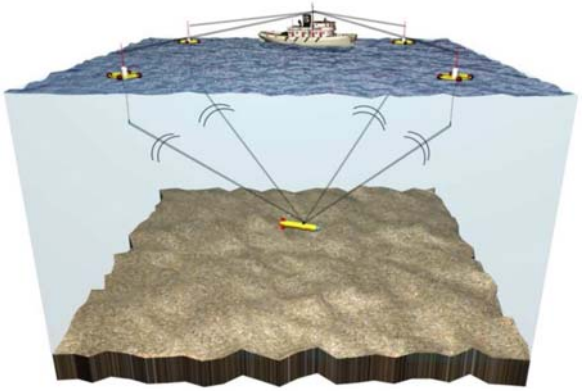

Fig. 2: A standard GIB scenario (from Alcocer (2009))

[1] This research was supported in part by the Collaborative Project 'MORPH' (N° 288704), founded by the 7th European Community Framework Programme.

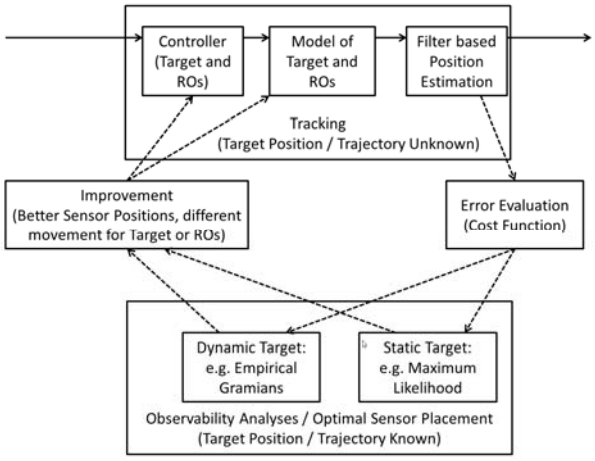

Fig. 3. The overall concept of Observability Analyses / Optimal Sensor Placement with respect to the Classical Estimation

and a number of ROs enable a position estimation or tracking of the target position by methods from estimation theory or filtering. Employments of these procedures led to the development of different solutions, like the so called GPS Intelligent Buoys (GIBs), where the roles of the ROs are adopted by surface buoys. Fig. 2 shows the principle setup. The concept which is explained in detail in Alcocer, Olivera and Pascoal, 2007 was further developed to replace the buoys with surface robots, e.g. for a diver assistant system (Glotzbach *et al.*, 2012).

2. BASIC TERMS, NOTATION, AND RELATION TO CURRENT STATE-OF-THE-ART

2.1 Optimal sensor placement in marine robotics

In marine navigation, optimal sensor placement comes more and more into focus (see e.g. the references below in this paragraph). Considering the acoustic range based methods as described above, the fact that small surface robots can play the role of the ROs expedites the need to find configurations in terms of numbers, positions and/or trajectories of the ROs that can be regarded as 'optimal' in some sense. Studies can be found in literature, that deal with optimal angular configuration of the sensors around the target (Martinez and Bullo, 2006), the optimal distance (Glotzbach *et al.*, 2013), or an optimal trajectory to employ only a single moving sensor (Moreno-Salinas, Pascoal and Aranda, 2013), employing methods based on the minimization of the determinant or trace of the Fisher Information Matrix for static target, to name but a few.

A unique property of these procedures is that the optimal configuration is a function of the overall setup as well as the target position which must be known in advance. Therefore, these studies are often criticized for being without practical use. This argument can be countered by the following arguments:

- This research is a first step into understanding the dependencies between general scenario setup, sensor positions and expectable results in terms of estimation error. When performing real sea trials, the need to face several real world problems like multi beam propagation or limited reliability and bandwidth of acoustic systems makes it reasonable to start with a scenario that is adapted to an 'optimal' configuration.
- In practical use, the overall process might be iterative, or the ROs might have to follow a moving target. Also, there are studies on scenarios where the target position is only known with some uncertainty, e.g. Isaacs, Klein and Hespanha, 2009. In these cases, the aiming for an optimal configuration at least with respect to the best current available estimation of the target position can be expected to improve the overall results.

Fig. 3 depicts the procedures of the classical estimation theory (above) and the efforts for improvement using Observability Analyses / Optical Sensor Placement (below). In the upper case, even if we consider that state of the art navigation algorithms in terms of filtering currently resort to Bayesian Estimation which uses prior knowledge on all estimated variables, the target position must be considered to be unknown or, to be more meticulous, to exhibit a very large level of uncertainty. In the lower case, it is aimed to improve the outcome of the estimation by computing optimal sensor positions, movement strategies for target and ROs, or other parameters (e.g. to which effect can the estimation result be improved if a certain state of the target can be measured), while the target position or trajectory is assumed to be known, with no or only small uncertainty.

2.2 *System Modelling and Mission Scenario*

We look at a scenario which is common for studies of navigation tasks based on acoustic range measurements in marine robotics and was used in previous works, e.g. Alcocer, Olivera and Pascoal, 2007 or Glotzbach *et al.*, 2012. We assume that an underwater agent, like a robot or a diver, is moving in a defined area, and its position shall be tracked by means of acoustic range measurements to ROs. The ROs are located at a position where they have full access to a global positioning system like GPS, and they are able to exchange data constantly. In the marine scenario, they are placed at the sea surface, and are in a constant contact with a computer which runs a model of the target to track. We will concentrate on scenarios with a single RO only that has to move in order to be able to observe the target position.

As the depth of the target can easily be measured by means of a standard depth cell, the tracking model is considered as a 2D kinematic model. We use the Random Walk with Constant Turning Rate (RWCTR), as described in Alcocer, 2009, both for target and RO. In this approach, the target is described by a state vector $\mathbf{x}$ with five states, namely the current position in a global coordinate systeme, x and y, magnitude and angle of the linear velocity vector in the xy-frame, v and ψ, and the rate of change of the letter one, r. Note that ψ might be different from the target's heading, as for marine vehicles heading and moving angle might differ. To enable the target to move on a path which is unknown to the tracker, no inputs are defined for the system, as it is unknown what the target does online. The possibility of the

target to change velocity, course angle and its rate is expressed by means of process noise ξ, which is assumed to be independent and identically distributed Gaussian with standard deviations σ_v, σ_ψ, and σ_r respectively. The discrete-time kinematic model is given by

$$\mathbf{x}(k+1) = \mathbf{F}(\mathbf{x}(k))\mathbf{x}(k) + \mathbf{G}\xi(k), \tag{1}$$

where

$$\mathbf{x}(k) := \begin{bmatrix} x(k) & y(k) & v(k) & \psi(k) & r(k) \end{bmatrix}^T$$

$$\mathbf{F}(\mathbf{x}(k)) := \begin{bmatrix} 1 & 0 & t_{step}\cdot\cos\psi(k) & 0 & 0 \\ 0 & 1 & t_{step}\cdot\sin\psi(k) & 0 & 0 \\ 0 & 0 & 1 & 0 & 0 \\ 0 & 0 & 0 & 1 & t_{step} \\ 0 & 0 & 0 & 0 & 1 \end{bmatrix}, \quad \mathbf{G} := \begin{bmatrix} 0 & 0 & 0 \\ 0 & 0 & 0 \\ 1 & 0 & 0 \\ 0 & 1 & 0 \\ 0 & 0 & 1 \end{bmatrix}$$

and

$$\xi(k) := \begin{bmatrix} \xi_v(k) & \xi_\psi(k) & \xi_r(k) \end{bmatrix}^T .$$

As we perform an observability analyses, we set the standard derivations for the process noise to 0. The model for the RO is similar; it additionally features two inputs for v and r to enable the control, and we let $\mathbf{x}_{\mathrm{RO}}$ represent the state vector for the RO to differentiate it from the target state vector.

The formulation of a realistic measurement model for the marine scenarios is sophisticated. One needs to take into consideration the runtimes of the acoustic signals, the delays caused by the modems, the relatively high error rate as well as the fact that when the RO receives an acoustic ping from the target, the target has already moved in the meantime. To address the latter, a back-and-forward approach as described for instance in Glotzbach *et al.*, 2012 can be employed. At this point, we will simplify the measurement model as much as possible, as our emphasis is on the observability analyses. We will assume that after every time instance t_{step}, a range measurement between target and RO is performed and is immediately available at the RO, that is,

$$\mathbf{y}(t_k) = \sqrt{(x(k) - x_{RO}(k))^2 + (y(k) - y_{RO}(k))^2} \, . \tag{2}$$

In simulation, the measurement is computed from the known positions of target and RO at the time of measurement. More details can be found in Section 4.

3. OBSERVABILITY ANALYSES AND EMPIRICAL GRAMIAN

The theory of observability of linear time-invariant systems is well known (see e.g. Rugh, 1996). This method cannot be directly extended to nonlinear systems, as the unobservable space depends on the actuator-sensor-configuration. The only existing result for the evaluation of local weak observability is given by Herman/ Krener, see Hermann and Krener, 1977. However, this is a sufficient condition, and it fails to provide any insight when the rank condition fails, and hence it requires further investigation. We resort to the method of the Empirical Gramian (see next paragraph and the references therein) in order to evaluate its usability to explore trajectories for RO that are rich in some sense for marine robot navigation.

Observability analysis proves which of the model states in $\mathbf{x}$ can be estimated from the system's measurement $\mathbf{y}$. For that purpose, the observability Gramian matrix $\mathbf{W}_O$ can be determined, which quantifies the generalized energy transfer E_O from the initial state $\mathbf{x}(0)$ to the output within an infinite time horizon for LTI-systems:

$$E_O = \int_0^\infty \mathbf{y}^T(\tau)\mathbf{y}(\tau)\,d\tau = \mathbf{x}^T(0)\,\mathbf{W}_O\,\mathbf{x}(0) \tag{3}$$

For the case of a nonlinear system as defined in (1), $\mathbf{W}_O$ can be approximated by the *empirical Gramian*, as suggested from Lall, Marsden, and Glavaški, 1999, and Hahn and Edgar, 2002. For that purpose the output $\mathbf{y}(t)$ has to be determined in a numerical simulation.

In advance, a nominal reference output trajectory $\mathbf{y}_0(t)$ is determined. For this purpose we use the initial state

$$\mathbf{x}_0 = \mathbf{x}_{\mathrm{nom}} \tag{4}$$

and solve the state differential equation by numerical integration to obtain the nominal output $\mathbf{y}_0(t)$ as a reference. Next, the initial conditions are modified by a number of $i_{\max}$ small perturbations $\Delta\mathbf{x}_i$

$$\mathbf{x}_{0,i} = \mathbf{x}_{\mathrm{nom}} + \Delta\mathbf{x}_i \tag{5}$$

with $i = 1, \ldots, i_{\max}$, and the corresponding outputs $\mathbf{y}_i(t)$ are determined again numerically. The perturbations are composed as:

$$\Delta\mathbf{x}_i = c\cdot\mathbf{S}\cdot\mathbf{t}_i^T \;\text{ with }\; \mathbf{S} = \mathrm{diag}(\mathbf{x}_{\max}) \tag{6}$$

Therein, the scalar constant $c \in [0\ldots1]$ is used to scale the amplitude within the maximum range specified by the diagonal matrix $\mathbf{S}$ that comprises the maximum value of each state. For small perturbations around the reference trajectory, e.g., $c = 0.01$ can be a good choice. The row vector $\mathbf{t}_i^T$ in $\mathfrak{R}^n$ is made up of combination of the elements −1 and +1. In order to cover all possible $i_{\max} = 2n$ combination in the sense of a full-factorial experimental design we choose

$$\begin{aligned} \mathbf{t}_1^T &= 1/\sqrt{i_{\max}}\begin{bmatrix} -1 & \ldots & -1 & -1 \end{bmatrix} \\ \mathbf{t}_2^T &= 1/\sqrt{i_{\max}}\begin{bmatrix} -1 & \ldots & -1 & +1 \end{bmatrix} \\ \mathbf{t}_3^T &= 1/\sqrt{i_{\max}}\begin{bmatrix} -1 & \ldots & +1 & -1 \end{bmatrix} \\ \mathbf{t}_4^T &= 1/\sqrt{i_{\max}}\begin{bmatrix} -1 & \ldots & +1 & +1 \end{bmatrix} \\ &\vdots \\ \mathbf{t}_{i_{\max}}^T &= 1/\sqrt{i_{\max}}\begin{bmatrix} +1 & \ldots & +1 & +1 \end{bmatrix} \end{aligned}$$

such that

$$\mathbf{T} = \begin{bmatrix} \mathbf{t}_1 & \ldots & \mathbf{t}_{i_{\max}} \end{bmatrix} \tag{7}$$

is an orthonormal matrix, and $\mathbf{T}\mathbf{T}^T = \mathbf{I}$ (Geffen *et al.,* 2008). The observability Gramian matrix $\mathbf{W}_O$ characterizes the energy transfer from initial states $\mathbf{x}_{0,i}(t)$ to the outputs $\mathbf{y}_i(t)$ in a neighborhood of the nominal trajectory $\mathbf{y}_0(t)$ within an infinite time horizon:

$$\mathbf{W}_{O,ij} = (c\mathbf{S})^{-1}\int_0^\infty \mathbf{t}_i^T\,\boldsymbol{\Psi}_{ij}(t)\,\mathbf{t}_j\,dt\,(c\mathbf{S})^{-1}, \tag{8}$$

with $\boldsymbol{\Psi}_{ij}(t) = \left[\mathbf{y}_i(t) - \mathbf{y}_0(t)\right]^T \cdot \left[\mathbf{y}_i(t) - \mathbf{y}_0(t)\right]$.

In total, the observability Gramian $\mathbf{W}_O$ is obtained from the superposition of the complete experimental design with $i, j = 1,\ldots, i_{\max}$.

For a sampled system with $t = t_{step} \cdot k$ of an finite horizon $t_{\text{final}} = t_{step} \cdot k_{\max}$, the empirical observability Gramian is

$$\mathbf{W}_{O,ij} = (c\mathbf{S})^{-1} \sum_{k=1}^{k_{\max}} \mathbf{t}_i^T \, \mathbf{\Psi}_{ij}(k) \mathbf{t}_j \, T_0 \, (c\mathbf{S})^{-1} \tag{9}$$

$$\text{with } \mathbf{\Psi}_{ij}(k) = \left[\mathbf{y}_i(k) - \mathbf{y}_0(k)\right]^T \cdot \left[\mathbf{y}_i(k) - \mathbf{y}_0(k)\right]$$

For nonlinear systems observability is not only a system property, but it also depends on the specific choice of inputs. A singular value decomposition of the empirical observability Gramian $\lambda(\mathbf{W}_O)$ allows assessing observability, as long as a 'typical' trajectory in the sense formulated in Lall, Marsden, and Glavaški, 1999, is used. The largest singular value $\lambda_{\max}(\mathbf{W}_O)$ rates the energy transfer from a single state with the best possible observability. On the other hand, the smallest singular value $\underline{\lambda}$ quantifies the energy transfer from the least observable state to the outputs. It characterizes the "bottleneck" of observability and will be considered in the following. A system is unobservable, if $\underline{\lambda}$ is zero.

It may not be necessary that all states are observable. If certain states are known from measurement or should not be estimated they can be excluded from the state vector. The remaining states that have to be observable are summarized in $\mathbf{x}_E$. For the tracking of an underwater target only its position is of interest and we select the first two states from the model in (1):

$$\mathbf{x}_E = (x \quad y)^T \tag{10}$$

To analyze the observability corresponding to the components of the state vector in $\mathbf{x}_E$, the rows and columns in $\mathbf{W}_O$ corresponding to those state variables not included in $\mathbf{x}_E$ are removed.

4. PATH PLANNING FOR A SINGLE RO

We consider the trajectory planning for a single RO by optimizing a measure of observability, according to last Section. We assume there are a target and one Reference Object. Both will be simulated using the RWCTR model as described in Section 2.2. We further assume that the RO is capable of measuring the range to the target every constant time interval according to the measurement model of Section 2.2. The target will either be stationary at the origin of a Cartesian coordinate system (Section 5.1) or move along a straight line which equals the x-axes of the coordinate system (Section 5.2). Our goal is to find a trajectory for the RO that is optimal in some sense with respect to the observability of the target position. In order to formulate a problem that is mathematically traceable, we need to discretise the control options of the RO. The controller can choose an action u from an admissible set U that will be used as initial condition for a time interval with n samples. The controller should maximize observability such that

$$u^* = \max_{u \in U} \left(\lambda_{\min}(\mathbf{x}_E)\right) \tag{11}$$

yields. Therefore, the time is divided into intervals with the length of T seconds. During T, the RO will be able to perform n range measurements to the target, one measurement every t_{step} seconds. During a time interval T, time t runs from t_0 to $t_0 + T$, the first measurement will be done at $t_0 + t_{step}$; the last one at $t_0 + T$. At the beginning of every time interval T, a control algorithm computes the values for velocity v and/or gradient of movement vector r (see Section 2.2), which will remain constant during the time interval T.

To find an optimal trajectory, the control algorithm can set r to either 0, or to a positive or negative value, $\pm \Delta r$. This results in three possible trajectories, as depicted in Fig. 4 a. For each trajectory, the positions where the RO will be when a range measurement will be performed can be computed (marked with small circles for one option in Fig. 4 a). For each trajectory and the corresponding measurement positions, the Gramian is computed according to (9), and the minimum eigenvalue for x- and y-position of the target is determined. The algorithm will then choose the trajectory with the largest minimum eigenvalue of $\mathbf{W}_0$.

Additionally, we also tried a more advanced algorithm that can also adapt the velocity. With the options to remain at the present velocity or to increase or decrease it by a predefined value Δv, and together with the three options for r, there were nine different trajectories to evaluate. We experienced that the algorithm always tried to raise the velocity to values that were much higher than the target velocity. As both objects are marine crafts, their velocities have to be in similar ranges. Therefore, we decided to use the simpler approach described above and to set the velocity of the RO to a constant value that is 2–3 times of the target velocity. An additional numerical simulation in order to find an optimal velocity is described in Section 5.3.

5. SIMULATIONS AND RESULTS

5.1 *Stationary Target*

A stationary target is placed at the origin of a Cartesian coordinate system. One RO is simulated according to the described RWCTR model, with an initial state vector of

$$\mathbf{x}_{init} = (-25 \quad 0 \quad 1.5 \quad 0 \quad 0)^T \, [\text{m} \quad \text{m} \quad \text{m/s} \quad ° \quad °/\text{s}]^T, \tag{12}$$

and Δr equals 0.1 °/s. The length of the time interval T was set to 10 s, with five range measurements (t_{step} = 2 s).

As described above, the RO evaluates three possible trajectories, as shown in Fig. 4 a. The trajectories themselves and the positions at which the range measurements would take place are computed and shown in the figure by circles. The measurement positions are used to determine the Empirical Gramian according to (9) for all three options. The option which results in the largest minimum eigenvalue will be realised. In the shown example and according to Table 1, this is the action 'left' (whereas the action 'right' option would result in the same eigenvalue, so one option needs to be preferred), which is marked with a solid line. At the end of

Table 1. Largest Minimum Eigenvalues of Empirical Gramian at selected time instances

	Time	Straight	Left	Right
Fig. 4 a	10 s	0,000	0,086	0,086
Fig. 4 b	20 s	0,782	0,546	0,990
Fig. 4 c	200 s	0,777	0,560	0,940

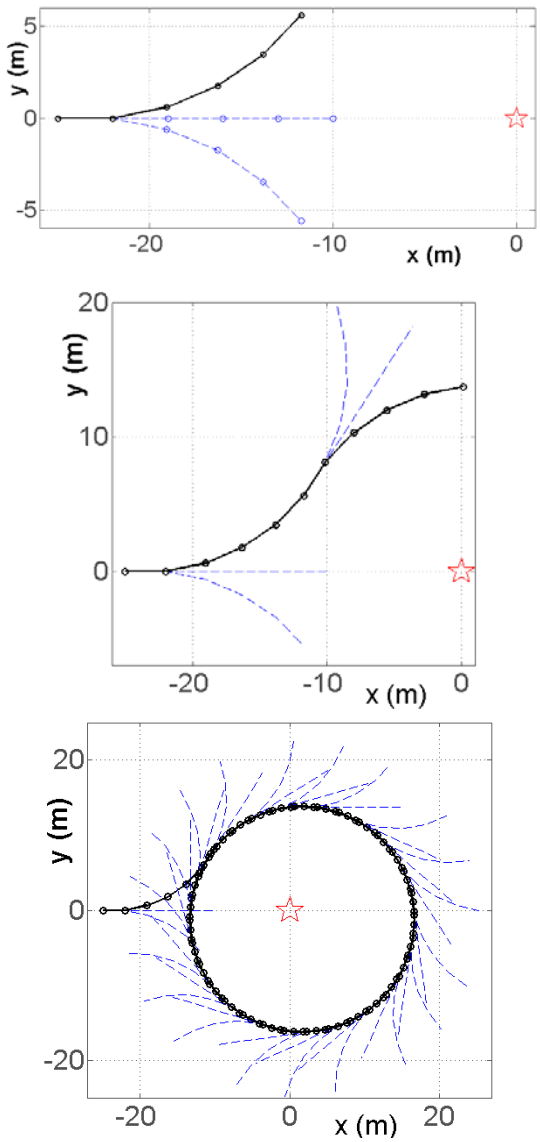

Fig. 4 a – c (top to bottom): Optimised trajectory for one RO; static target position marked by star.

the current time interval, the process is redone, shown in Fig. 4 b. From now on, the measurement positions are only shown in the figures for the option that was finally selected. For the second evaluation, the action 'right' is chosen (see also Table 1). In any further evaluations, always the action 'right' will deliver the best result; the RO moves on a circle around the target in a clockwise direction. Fig. 4 c depicts the situation after three turns are executed. The target, marked as a star, is not in the centre point of the circle, which may be due to the discretized control options of the RO.

It shall be noted at this point that the values for the parameters were chosen both to be in realistic ranges for maritime robots (e.g. concerning velocity) and to produce demonstrative results. E.g., the relation between T and Δr was chosen to allow the RO to turn for about 45 degrees in one time interval. Different employed settings resulted in less demonstrative results which might need more time to converge to a stable situation, but at the end the RO was always moving on a trajectory which looped around the target.

It is interesting to compare this result with another one from Literature. In Moreno-Salinas, Pascoal, and Aranda, 2013, the authors also investigated an optimal trajectory for a single RO and a static target. Their methodology was to trace back the problem to the optimal placement of several (static) ROs (by employing the Maximum Likelihood method) and to make the single RO to choose a trajectory through the computed positions. In their example, the RO was approaching the target and also ended up circling around it. It is worth to mention that the different two employed methodologies led to the same result.

5.2 *Moving* Target

In a second mission scenario, the target is moving along the x-axis of the coordination system. Its initial state vector is set to

$$\mathbf{x}_{init} = (0 \quad 0 \quad 0.5 \quad 0 \quad 0)^T [\text{m} \quad \text{m} \quad \text{m/s} \quad ^\circ \quad ^\circ/\text{s}]^T . \tag{13}$$

All other parameters are the same as for the scenario described in Section 5.1, except for the constant velocity of RO, which was reduced to 1.2 m/s.

Fig. 5 a–c show the trajectory generated by the described algorithm. The RO moves parallel to the trace of the target, uses its higher velocity to overtake it and performs a circular movement around it. This behaviour is repeated, resulting in a Pretzel-shaped trajectory. The values of the largest minimum eigenvalues for the time instances shown can be found in Table 2.

Table 2. Largest Minimum Eigenvalues of Empirical Gramian at selected time instances

	Time	Straight	Left	Right
Fig. 5 a	130 s	0,953	0,728	1,145
Fig. 5 b	360 s	0,042	0,025	0,049
Fig. 5 c	970 s	0,019	0,017	0,015

Engel and Kalwa, 2009, were investigating a similar problem, where two cooperative marine vehicles were intended to perform relative navigation based on range measurements. Exploiting the Hermann-Krener rank condition for local week observability (see Hermann and Krener, 1977 for details), they concluded that a situation where one vehicle is circling around the other one yields an extreme case for satisfied local observability condition. It is worth mentioning that our employed approach with Empirical Gramians generates a similar trajectory.

5.3 *Investigation on optimal velocity*

As it was stated in Section 4, the scenario used here is of very theoretical nature. Therefore, we set T to 1 s and t_{step} to 0.1 s, without adding an upper limit for the velocity of the RO. These values are not realistic for marine robots and acoustic range measurements; the intention is to get a general understanding of a theoretical velocity optimization.

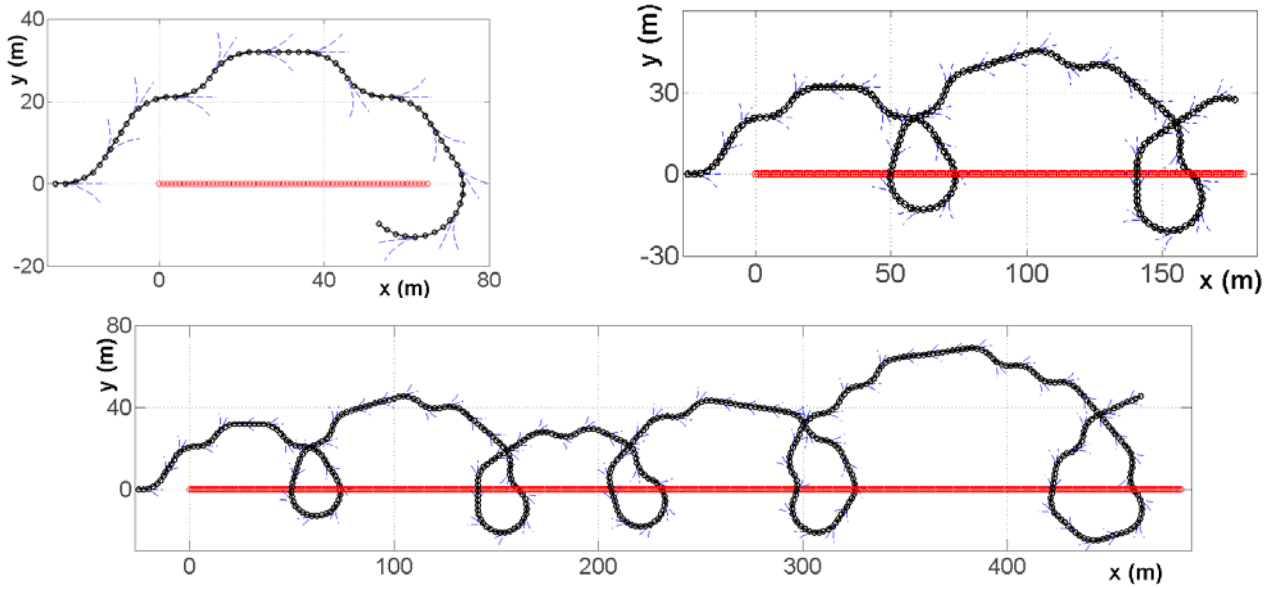

Fig. 5 a – c (left to right, top to bottom): Optimised trajectory for one RO; trace of moving target (in positive x direction) marked by circles.

We consider that the RO has to move on the circumference of a circle with a fixed radius r_0 of 10 m (arbitrarily chosen) around the position of the stationary target. The RO is capable of changing its velocity v. At the same time, it always has to adapt its gradient of moving vector r in order to stay on the circumference. The utilized algorithm is omitted at this place due to space limitations. The changes of velocity are realized by a similar algorithm as presented in Section 4. At the beginning of each time interval T, three possible trajectories for the next T seconds are evaluated: keeping the current velocity or increasing or decreasing it by a defined amount, Δv. An example is shown in *Fig. 6*. The RO starts at position (–10, 0) m at the beginning of T and moves counterclockwise. Maintaining at the current velocity of 20 m/s would result in the green trajectory, where the asterisks mark the range measurement positions. The control algorithm also has the options to increase or decrease the velocity by 3 m/s, which results in the blue trajectory with the triangle-markers, or the brown trajectory with the diamond markers, respectively. According to (9), the algorithm chooses the option that generates the largest minimum eigenvalue of the Empirical Gramian, which is the option that increases the velocity, see Table 3

We initialized our simulations with a starting velocity of 1 m/s and a Δv of 1 m/s. The controller increased the velocity to a value of 31 m/s and maintained there. To improve the result, we performed a second run with a starting velocity of 31 m/s and a Δv of 0.001 m/s. The velocity was raised to and maintained at a final value of 31.416 m/s. Note that, for $T = 1$

Table 3: Largest Minimum Eigenvalues of Empirical Gramian at selected time instances

	Time	Increase	Maintain	Decrease
Fig. 6	1 s	0,34	0,27	0,21
Fig. 7	417 s	0,499983	0,499999	0,499985

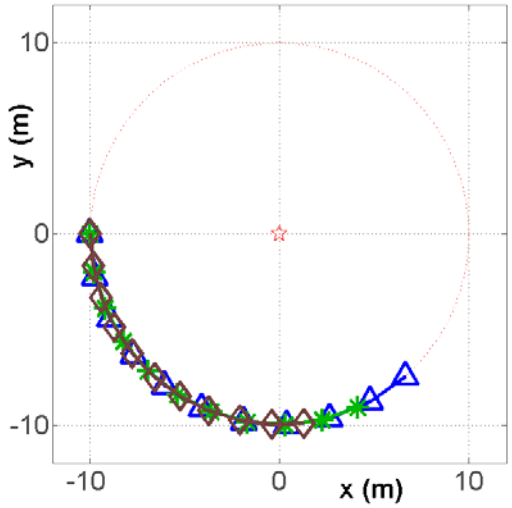

Fig. 6: Possible trajectories for RO around the target position (marked by the red star)

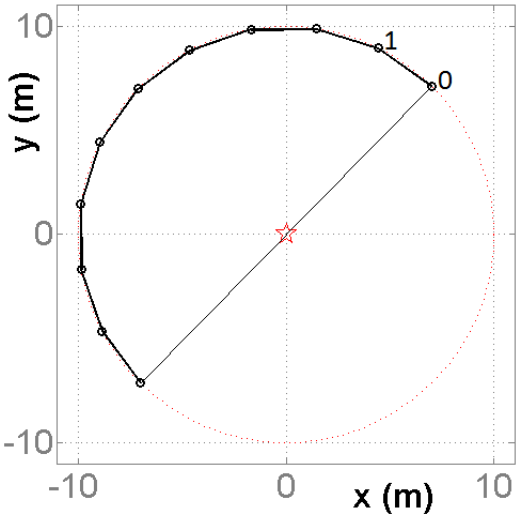

Fig. 7: Trajectory after the final velocity is reached

s and radius r_0 = 10 m, that means that during one time interval T, the RO is moving along half the circumference of the circle (r_0 times π). Fig. 7 shows a trajectory for one time interval T after the final velocity is reached. Note that the first marker (tagged as 0) is the starting position at which no measurement takes place in the current interval. The following 10 markers show the positions at which measurements will be performed. In Table 3, it becomes obvious that maintaining the velocity is the best option.

It is interesting to compare these results with those presented by Martinez and Bullo, 2006, for non-marine scenarios. They were seeking optimal angular configurations for a number of n range measuring devices to be placed on a convex structure around the target position, employing the Maximum Likelihood procedure. They proofed that the placement of the n sensors at positions on the circumference of a convex object surrounding the target with the polar coordinates

$$\eta_i = (i-1)\pi/n, \quad i \in \{1,...,n\} \tag{14}$$

for the sensors yields an optimal solution. Our optimal solution in Fig. 7 corresponds exactly to this equation, if we start counting at the first measurement position (marker 1).

6. CONCLUSIONS

We employed the Empirical Gramian approach to investigate observability properties and to compute optimal trajectories for a range-measuring Reference Object in several simplified mission scenario inspired by application from marine robotics. For three different situations, we could achieve similar results as in other papers from literature, where different methodologies were employed. We believe that our results are of practical use, especially in comparison to the two other methods presented. Using the Herman/ Krener rank condition, it can only be evaluated whether a system is locally weak observable or not; there is no way to compare several solutions that are observable in order to find an optimal one. Using the Maximum Likelihood Method, an optimal configuration can be computed, however, there is no guarantee that a specific marine vehicle used as RO features the necessary manoeuvrability to execute the calculated trajectory. The convenience of the method proposed in this paper is that the manoeuvrability of the RO can be considered right from the beginning by only using executable trajectories for the optimization progress. Furthermore, the Empirical Gramian method is based on a dynamical system model, which might be more realistic if the target is considered to be moving.

Therefore, the Empirical Gramians can be seen as a promising option for the usage in marine robotics, as it can easily be implemented into the existing control hardware. Future research activities will aim to realise applications of Empirical Gramians in real sea trials to further validate its usability.

REFERENCES

Alcocer, A., P. Oliveira and A. Pascoal (2007). Study and implementation of an EKF GIB-based underwater positioning system. In *Control Engineering Practice*, **Volume 15**, Issue 6, June 2007, Pages 689–701.

Alcocer, A. (2009). Positioning and Navigation Systems for Robotic Underwater Vehicles. *PhD Dissertation thesis of the Instituto Superior Técnico, Lisbon*, October 2009.

Engel, R. and J. Kalwa (2009). Relative positioning of multiple underwater vehicles in the GREX project. In: CD-ROM-Proceedings of IEEE OCEANS ´09, Bremen, Germany.

Geffen, D., R. Findeisen, M. Schliemann, F. Allgöwer and M. Guay (2008). Observability Based Parameter Identifiability for Biochemical Reaction Networks. In: *Proceedings of the American Control Conference*, 2130–2135.

Glotzbach, Th., M. Bayat, A.P. Aguiar and A. Pascoal (2012). An Underwater Acoustic Localisation System for Assisted Human Diving Operations. In: *9th IFAC Conference on Manoeuvring and Control of Marine Craft (MCMC), 2012*, Arenzano, Italy, no pagination.

Glotzbach, Th., D. Moreno-Salinas, A. Pascoal and J. Aranda (2013). Optimal Sensor Placement for Acoustic Range-Based Underwater Robot Positioning, In: *9th IFAC Conference on Control Applications in Marine Systems (CAMS), 2013*, Osaka, Japan, no pagination

Hahn, J. and T.F. Edgar (2002). An improved method for nonlinear model reduction using balancing of empirical gramians. In: *Computers and Chemical Engineering* **26**, 1379-1397.

Hermann, R. and A.J. Krener (1977). Nonlinear Controllability and Observability. In: *IEEE Transactions On Automatic Control*, **Vol. AC-22, No. 5**, October 1977, pp. 728-740.

Isaacs, J.T., D.J. Klein and Hespanha, J.P. (2009). Optimal Sensor Placement For Time Difference of Arrival Localization, In: *Conference on Decision and Control, 2009* held jointly with the *2009 28th Chinese Control Conference (CDC/CCC 2009)*, pp. 7878-7884

Kalwa, J., A. Pascoal, P. Ridao, A. Birk, M. Eichhorn, L. Brignone, M. Caccia, J. Alves and R.S. Santos (2012). The European R&D-Project MORPH: Marine robotic systems of self-organizing, logically linked physical nodes. In: *9th IFAC Conference on Manoeuvring and Control of Marine Craft (MCMC), 2012*, Arenzano, Italy, no pagination.

Lall, S., J.E. Marsden and S. Glavaški (1999). Empirical model reduction of controlled nonlinear systems. In: *Proceedings of the IFAC World Congress*, 473-478.

Martínez, S. and F. Bullo (2006). Optimal sensor placement and motion coordination for target tracking, In: *Automatica* **42**, p. 661 – 668.

Moreno-Salinas, D., A. Pascoal and J. Aranda (2013). Underwater Target Positioning with a Single Acoustic Sensor. In: *9th IFAC Conference on Control Applications in Marine Systems (CAMS), 2013*, Osaka, Japan, no pagination.

Rugh, W.J. (1996). *Linear Systems Theory*. Prentice Hall Publications, London, 1996.